Pak. J. Bot., 57(5): 1861-1872, 2025. DOI: http://dx.doi.org/10.30848/PJB2025-5(20)

RUMEX NERVOSUS VAHL INDUCES APOPTOSIS AND SUPPRESSES VEGFA IN HEPATOCELLULAR CARCINOMA (HEPG2) CELLS

ABDULRAHMAN ALASMARI

Department of Biology, Faculty of Science, University of Tabuk, Tabuk, 71491, Saudi Arabia
Biodiversity Genomics Unit, Faculty of Science, University of Tabuk, 71491, Tabuk, Saudi Arabia
Corresponding email: ab.alasmari@ut.edu.sa

Abstract

This study investigates the apoptotic and anti-angiogenic role of *Rumex nervosus (R. nervosus)* ethanol extraction on human hepatocellular carcinoma (HepG2) cell. The MTT test confirmed the cytotoxicity nature of *R. nervosus* with an IC_{50} value of 14µg/mL, while the trypan blue exclusion assay further demonstrated the induction of apoptotic cells. The fluorescence staining test revealed that dead bodies by AO/EtBr and DCFH-DA analysis enumerated the accumulation of ROS in HepG2 cells. Additionally, *R. nervosus* treatment compromised mitochondrial function, as indicated by Rho-123 staining, and caused loss of nuclear integrity, evidenced by Hoechst 33342 staining. FDA staining further confirmed reduced cell viability due to diminished esterase activity Functional assays, including colony formation, invasion, and migration, showed a significant reduction in cell mobility, invasion capability, and colony-forming potential following *R. nervosus* exposure. qRT-PCR analysis elucidated the upregulation of pro-apoptotic genes (such as caspase-3, caspase-8, caspase-9, and cytochrome c), along with downregulation of anti-apoptotic genes like Bcl-2. Western blot analysis validated the downregulation of VEGFA, HIF-1α, and p-Akt, and the upregulation of cleaved PARP and cytochrome c. Altogether, *R. nervosus* induces apoptosis and angiogenesis suppression in HepG2 cells through the arrest Pi3K/Akt pathway by augmenting the ROS generation with loss in mitochondrial membrane potential (ΔΨm). These findings suggest that *R. nervosus* holds potential as a therapeutic agent for hepatocellular carcinoma.

Key words: *Rumex nervosus;* Apoptotic and anti-angiogenic; HepG2; Gene expression.

Introduction

Cancer is a life-threatening disease characterized by uncontrolled cell proliferation. Hepatocellular carcinoma (HCC), a common form of liver cancer, poses a significant health risk due to its aggressive nature. In 2021 alone, there were 9.05,677 newly diagnosed cases of liver cancer worldwide (Sung *et al*., 2021). One critical factor in cancer progression is pathological angiogenesis, where tumors develop new blood vessel formation under nutrient stress (Khadka *et al*., 2023) or hypoxic conditions (Krock *et al*., 2011) by secreting VEGF cytokines. This process facilitates tumor growth, relapse or metastasis.

A promising therapeutic strategy for cancer treatment is the induction of apoptosis or programmed cell. Apoptosis is regulated by many signaling proteins, including poly (ADP-ribose) polymerase (PARP). The cleaving of PARP might arrest the DNA repairing and causes DNA fragmentation (Agarwal *et al*., 2009). More on, the cell survival pathway signaling Pi3K/Akt enhances the lifespan of cells and is involved in the proliferation and cancer-related cellular functions (Zhou *et al*., 2017). On another side, disruption in the electron transport chain is paid great attention to inducing apoptosis in cancer treatment. On this axis, the loss of mitochondria membrane potential allows the translocate of cytochrome c to the cytoplasm. As a result, defect in the electron passing in the electron transport chain (ETC) and a deficiency in the ATP production (Rohlena *et al*., 2013). Combining apoptosis induction with angiogenesis suppression offers a potent strategy for effective cancer treatment. Conventional therapies like chemotherapy, surgery, and radiation often come with significant side effects. Therefore, the development of new treatments from natural sources is essential for safer and more effective cancer management.

Medicinal plants are a rich source of bioactive phytochemicals and multiple phytochemicals by the herbal plants produce significant results in clinical trials of cancer patients (Hosseini & Ghorbani, 2015). Taken into account, the Rumex genus, belonging to the Polygonaceae family which consists of more than 250 species known for their medicinal properties (Alwashli *et al*., 2012). Different parts of rumex plants are utilized for medicinal values including diabetes mellitus, hypertension, wounds, constipation, diarrhea, and inflammation that are demonstrated by the anti-microbial, anti-inflammatory, anti-oxidant, anti-parasitic, diuretics, and analgesic potential (Alwashli *et al*., 2012; Qasem *et al*., 2020). In the close view of rumex plants, *Rumex nervosus* (*R. nervosus*) is a common species found in the Arabian and African countries. In countries like Saudi Arabia and Yemen, the leaves of *R. nervosus* are used to enhance wound healing properties and treat inflammation or skin diseases (Getie *et al*., 2003; Rahman *et al*., 2007; Al Yahya *et al*., 2018).

Extract of *R. nervosus* exhibited a range of medicinal benefits, including anti-obesity, anti-diabetes, hypolipidemic, anti-inflammatory, and free radical scavenging activities (Desta *et al*., 2016; Quradha *et al*., 2019). Prolonged use of *R. nervosus* has been shown to effectively reduce hyperglycemia, and hyperlipidemia (Al-Naqeb & Deen, 2017). Studies also sugges that *R. nervosus* can inhibit inflammation by suppressing NF-κB, nitric acid synthase, and cyclooxygenase activity (Desta *et al*., 2016; Quradha *et al*., 2019).

Despite these promising medicinal properties, research on the anti-cancer properties of *R. nervosus* remains limited. Preliminary studies have indicated cytotoxicity effects, but detailed molecular insights are lacking. In the present study, we tested the anti-cancer molecular insights of ethanol extract of *R. nervosus* focusing on its ability to induce

apoptosis and suppress angiogenesis-related gene expression, particularly VEGFA, in HepG2 liver cancer cells. This is the first study to explore these molecular pathways, providing new insights into the potential use of *R. nervosus* as a natural anti-cancer agent.

Material and Methods

Chemicals: The cell culture required chemicals such as DMEM, antibiotics, and FBS were purchased from Himedia, Mumbai (India). Fluorescence dyes such as acridine orange, ethidium bromide, Rho-123, DCFH-DA, FDA, and Hoechst-33342 are acquitted from the Thermo Fisher Scientific Company (USA). The blotting technique required chemicals procured from cell signaling technologies, USA.

Cell culture: HepG2 cancer cells were purchased from the NCCS, Pune, India, and cultured under humidified environment (37˚C/ 5% CO_2) using the DMEM culturing medium with supplementation of 10% FBS and 1% streptomycin/penicillin. The normal liver cells (THLE-2) were purchased from the ATCC, USA, and maintained under a specific protocol provided by ATCC.

Collecting, identification, and production of an ethanol extract from the plant: The ethanol extract of the *R. nervosus* plant was used to identify the apoptotic-inducing ability on HepG2 cells. The plant leaves were pounded into a fine powder after being dried for seven days in the dark. A 100 g sample of fine powder was subjected to soxhlet with ethanol. The extract was lyophilized and placed in a storage container at -80°C until use.

Cytotoxicity assay (MTT- Test): The MTT experiment was used to calculate the IC_{50} value of the ethanol extract of *R. nervosus*. HepG2 and THLE-2 cells (1×10^4 cells/well) were seeded in 96 multi-well plates. After 24 hours, the culture medium was replaced with fresh DMEM containing various concentrations of the extract. Following a 24-hour incubation, a 20 µl of MTT substrate (5 mg/1 mL of 1×PBS) was added to each well and incubated for 4 hours. The formazan crystals were dissolved in 200 µl of DMSO and absorbance was measured at 595 nm using a multi-well plate reader. The following formula was used to generate the cell viability graph,

$$\% \text{ Of cell viability} = \frac{\text{OD of the sample}}{\text{OD of the control}}$$

Trypan blue exclusion method: The trypan blue exclusion test was used in the study to evaluate apoptotic cells. In a brief, HepG2 cells were seeded (1×10^5 cells/well) and exposed to *R. nervosus* for 24 and 48 hours. Cells were trypsinized and pelleted the next day. Trypan blue was used in the cell counting chamber to count the collected cells. The apoptotic graph was plotted after the number of apoptotic cells was determined.

Cell viability test: Cell viability was also confirmed using the MTT assay. HepG2 cells were treated with different concentrations of *R. nervosus* (0, 20, and 40 g) for varying periods (0, 12, 24, and 48 hours) to assess the extract's impact on cell viability.

Morphology observation: The cells' morphological changes were observed using phase-contrast microscopy. HepG2 cells were treated with varying concentrations of *R. nervosus* for different time intervals. Images were captured using Floid microscopy (Life Technology, USA) at 20× magnification.

Live/dead assay (AO/EtBr): Fluorescence microscopy was used to examine the Live/Dead material to determine the influence of *R. nervosus*. In a word, 1×10^5 HepG2 cells were plated on six-well plates and given the night to mature. Moreover, *R. nervosus* was applied to cells for 24 and 48 hours. Cells were then treated in AO/EtBr dual staining solution for 10 min in a dark environment after the treatment. The plate was subsequently examined using fluorescence microscopy with a 20× field of view (Accu-Scope, EXI-310, USA), and pictures were recorded.

ROS detection (DCFH-DA method): Using the DCFH-DA dye technique, intracellular-produced ROS were measured. HepG2 cells (1×10^5 cells) were first seeded on the six-well plate. Using the IC_{50} value as a guide, the cells were cultured under the *R. nervosus* for 24 and 48 hours after cell maturation. The plate was properly processed after the treatment by adding DCFH-DA solution and allowing it to stand for 30 minutes in a dark room. A liquid layer was also taken off the plate, and it was then examined with a green filter by the Accu-Scope, EXI-310, USA. The recorded photos were the last step in the process.

Mitochondrial membrane potential assay (ΔΨm): Mitochondrial membrane potential was evaluated using Rho-123 staining. *R. nervosus* was either added to or left out of 1×10^5 HepG2 cells that had been seeded deeply on a six-well plate for 24 and 48 hours. The procedure was completed by washing the cells in 1×PBS and staining them with Rho-123. The plate was continuously exposed to darkness for 15 minutes. The plates were then examined under a green light after the extra dye had been removed. The photos were taken using fluorescence microscopy (Accu-Scope, EXI-310, USA).

DNA fragmentation assay (Hoechst-33342): DNA fragmentation was detected using Hoechst (33342) staining technique. In an essence, the HepG2 cells were planted on six-well plates and left in an incubator overnight. The next day, cells were treated with or without *R. nervosus* for 24 and 48 hours. The plate was then prepared for the following step and incubated with Hoechst dye for 15 min in the dark. The plate was examined in a blue filter with a 20× magnification field (Accu-Scope, EXI-310, USA).

FDA test: The cell viability-specific dye fluorescein diacetate (FDA) was used to measure the cell viability. In turn, HepG2 cells were seeded on six-well plates at 1×10^5concentration. The next day, cells were treated at IC_{50} value of *R. nervosus* for 24 and 48 hours. After that, FDA dye was added and incubated under dark conditions for 15 minutes. Later, the green filter was used to analyze the viability of *R. nervosus* treated HepG2 cells under fluorescence microscopy, at Accu-Scope, EXI-310, USA.

Wound-Closure assay: Cell migration was assessed using a wound-healing assay. A sterile pipette tip was used to scratch a monolayer of HepG2 cells. The cells were then treated with *R. nervosus* and monitored over time using fluorescence microscopy (Accu-Scope, EXI-310, USA).

Transwell migration assay: The matrigel-coated Transwell migration insert chamber was employed to examine the characteristics of cell invasion. In a nutshell, the upper portion of the chamber was covered with Matrigel (2 mg/mL, BD Biosciences). *R. nervosus* was used to treat the HepG2 cells that were placed on top of the transwell chamber. In the middle of the treatment hour, 10% FBS was added to the chamber's bottom. Methanol was used to fix the invading cells from the upper portion of the compartment (20 minutes fixation). Crystal violet solution diluted to 0.1% is used to stain the fixed cells. Light microscopy is used to count the invading cells in a 20× magnification field.

Colony formation assay: The capacity to establish colonies was crucial in the tumor relapse condition. We carried out colony formation using crystal violet staining in consideration of this. Cells were collected and cultivated again for 15 days after being exposed to *R. nervosus* without being disturbed. Later, formed colonies are counted after already being stained with 0.1% crystal violet staining. The graph was then plotted by counting colonies.

qRT-PCR analysis for mRNA expression: The apoptotic network gene expressions were identified by the qRT-PCR study. The TRIzol technique was used to separate the total RNA from the *R. nervosus*-treated and untreated HepG2 cells. The complementary DNA was constructed (cDNA synthesis kit, TAKARA, 6110A) using 2 µg of total RNA, and the syber green solution was utilized to find out the exact gene expression (Used primers listed in Table 1). The internal control was achieved by the level of Beta-Actin level. Using the $2^{-\Delta\Delta ct}$ approach, the relative quantitative gene expression was determined.

Western blot technique: This study used immunoblot analysis to pinpoint the expression of a particular protein. Briefly, using the RIPA buffer technique, complete cellular proteins were extracted after cells were treated with or without an IC50 value of *R. nervosus*. The protein was then measured using Lowry's technique (Lowry *et al*., 1951). For protein separation, an equivalent protein concentration was then injected onto an SDS-PAGE gel. After SDS running, the gel was then exposed to the nitrocellulose membrane-based protein transfer technique. An overnight incubation with a particular primary antibody has been added to the membrane. A secondary antibody was then applied to the membrane and left on it for four hours. The membrane was then given a moderate wash before being given a minute to react with the BCIP/NBT substrate.

Significance analysis: The mean and standard deviation (mean± SD) for each result was displayed. When ****$p<0.0001$, ***$p<0.001$, **$p<0.01$, *$p<0.05$, and *ns* were present, the p-value was deemed statistically significant. To determine the difference in significance between the groups, one-way and two-way ANOVA were used.

Results

***R. nervosus* causes toxicity to HepG2 cytoplasm:** The anti-cancer potential of ethanol extract *R. nervosus* was tested by the MTT method. In turn, the obtained results revealed that significantly causes the cytotoxicity at 14 µg/ mL for the HepG2 cells in 24 hrs. In contrast, the normal liver cells THLE-2 shows the IC_{50} value at 18 µg/ mL for 24 hrs. In addition, the MTT data suggest that increasing the concentration of *R. nervosus* induces consistent cell viability loss in HepG2 and THLE-2 cells (Figs. 1a and b). The obtained data shows that *R. nervosus* effectively induces cell viability loss in HepG2 cells and further experiments adopted the same cells.

***R. nervosus* generates apoptotic cells:** For the confirmation of cell viability loss, this study performs the trypan blue exclusion method. Briefly, the different experiment time points (0, 24, and 48 hrs) were followed, and collected data enforced that 24 and 48 hrs of *R. nervosus* administration induces cell apoptosis significantly when compared with 0 µg and 0 hrs. The obtained data depicts that *R. nervosus* serves as a cytotoxicity source for Hepg2 cells (Fig. 1c).

***R. nervosus* significantly decreases cell viability in HepG2 cells:** The sustained cytotoxicity potential of *R. nervosus* was further assessed at 0, 12, 24, and 48 hours using the MTT assay. The results demonstrated that increasing the concentration and exposure time *R. nervosus* suppressed HepG2 cell growth progressively. The obtained data robustly stated that *R. nervosus* effectively works against the HepG2 cells (Fig. 1d).

Table 1. Primers were used in this study.

S. #	Gene	Forward primer	Reverse Primer
1.	Actin-B	F:5'-TGAAGGCTTTTGGTCTCCCTG -3'	R:5'-ACAAAGTCACACTTGGCCTCA -3'
2.	Caspase-3	F:5'-TCCTAGCGGATGGGTGCTAT -3'	R:5'-CTCACGGCCTGGGATTTCAA -3'
3.	Caspase-8	F:5'-TTCAGACTGAGCTTCCTGCC -3'	R:5'-GACCAACTCAAGGGCTCAGG -3'
4.	Caspase-9	F:5'-AGGCCCCATATGATCGAGGA -3'	R:5'-GGCCTGTGTCCTCTAAGCAG -3'
5.	BCL2	F:5'-F-AAAAATACAACATCACAGAGGAAGT -3'	R:5'-GTTTCCCCCTTGGCATGAGA -3'
6.	Bax	F:5'-GGAGCAGCCCAGAGGC -3'	R:5'-TTCTTGGTGGACGCATCCTG -3'
7.	BID	F:5'-TGGGAGACGCTGCCTCG -3'	R:5'-GGAACCGTTGTTGACCTCAC -3'
8.	CYCS	F:5'-TCGTTGTGCCAGCGACTAAA -3'	R:5'-ACCATGGAGATTTGGCCCAG -3'
9.	PTEN	F:5'- AGGGACGAACTGGTGTAATGA -3'	R:5'- GGGAATAGTTACTCCCTTTTTGTCT -3'
10.	PI3K	F:5'-CCCGATGCGGTTAGAGCC -3'	R:5'-TGATGGTCGTGGAGGCATTG -3'
11.	Akt	F:5'-CAGGATGTGGACCAACGTGA -3'	R:5'-AAGGTGCGTTCGATGACAGT -3'
12.	PARP	F:5'-CGCCTGTCCAAGAAGATGGT -3	R:5'-CTGACTCGCACTGTACTCGG -3'

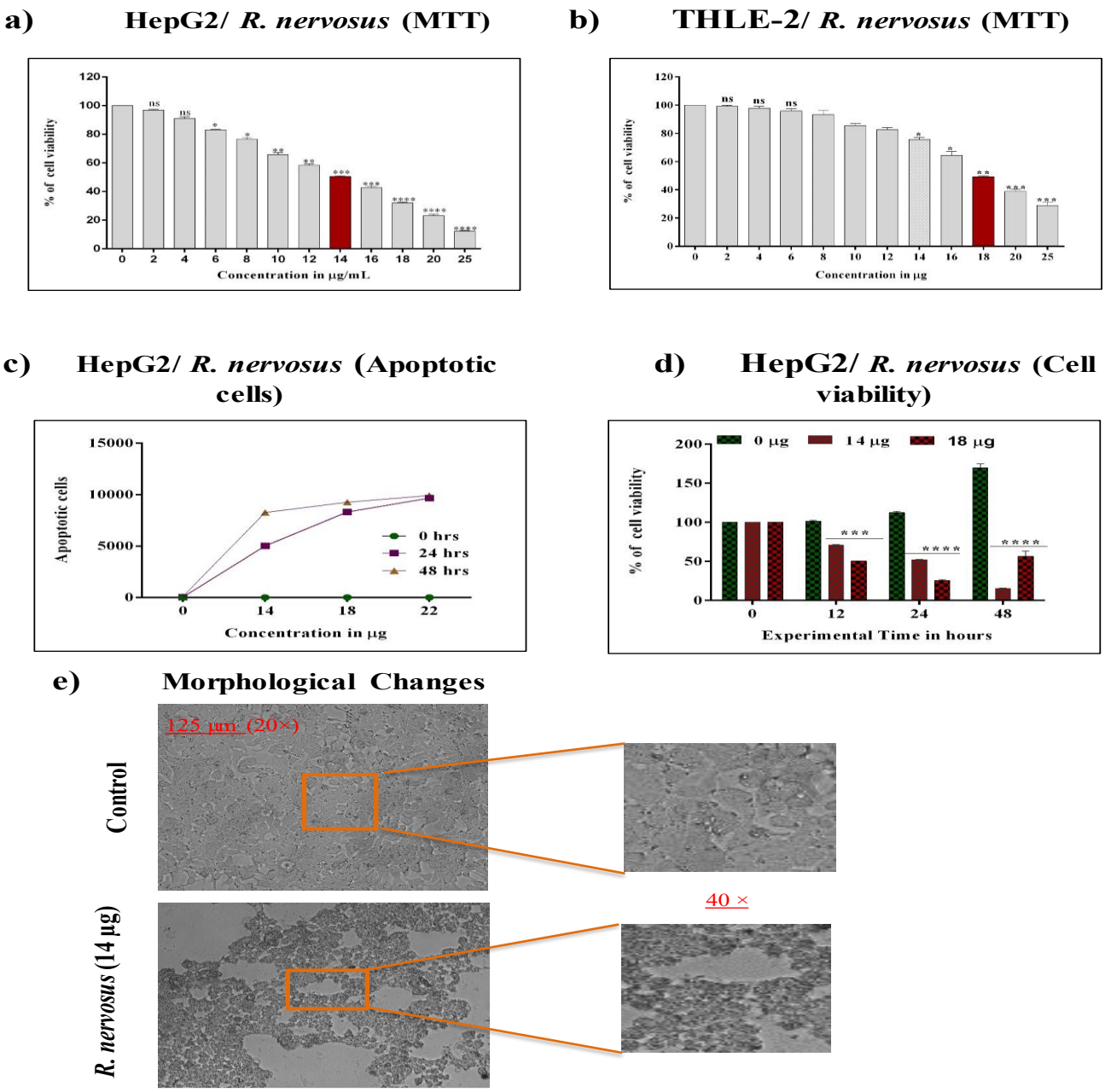

Fig. 1. *R. nervosus* induces cytotoxicity HepG2: a) Shows the *R. nervosus* induced cytotoxicity in HepG2 cells. b) The normal liver cell THLE-2 compatible against the plant extract of *R. nervosus*. c) Graph illustrated the produced apoptotic cell by trypan blue exclusion method. d) Time and dose depended on an analysis of cell viability of HepG2 cells against *R. nervosus*. e) Monolayer-morphology analysis of HepG2 under *R. nervosus*. All quantified values represent mean ± SD. Statistical significance is performed by one-way ANOVA followed by Dunnett's multiple comparison test.Values are statistically significant at ****p<0.0001, ***p<0.001, **p<0.01, *p<0.05, and *ns*.

***R. nervosus* disturbs HepG2 morphology:** Morphological observations of the HepG2 monolayer revealed that untreated cells maintained a healthy, proliferative appearance. In contrast, *R. nervosus*-treated cells displayed disrupted monolayers with increased cell damage and reduced cell population. This observation depicts *R. nervosus* as capable to induce disturbing the HepG2 monolayer (Fig. 1e).

***R. nervosus* produces dead cells in HepG2:** The *R. nervosus* effectively produces dead cells in HepG2 cells that were determined by the AO/EtBr dual staining method. The control cells exhibit compact nuclei with significant emission of green fluorescence. In the case of treated cells, half of the cells died and emit the red color and the remaining cells emitted the green fluorescence under 24 hrs treated HepG2 cells. In addition, the used IC_{50} values perfectly kill maximum cells at an extended time duration (48 hrs treatment) (Fig. 2a).

***R. nervosus* induces the accumulation of ROS:** Intracellular ROS levels were measured using the DCFH-DA assay. Control cells exhibited minimal ROS emission, while *R. nervosus*-treated cells showed significantly higher ROS levels. ROS accumulation was greater at 48 hours than at 24 hours (Fig. 2b), highlighting the role of oxidative stress in *R. nervosus*-induced apoptosis.

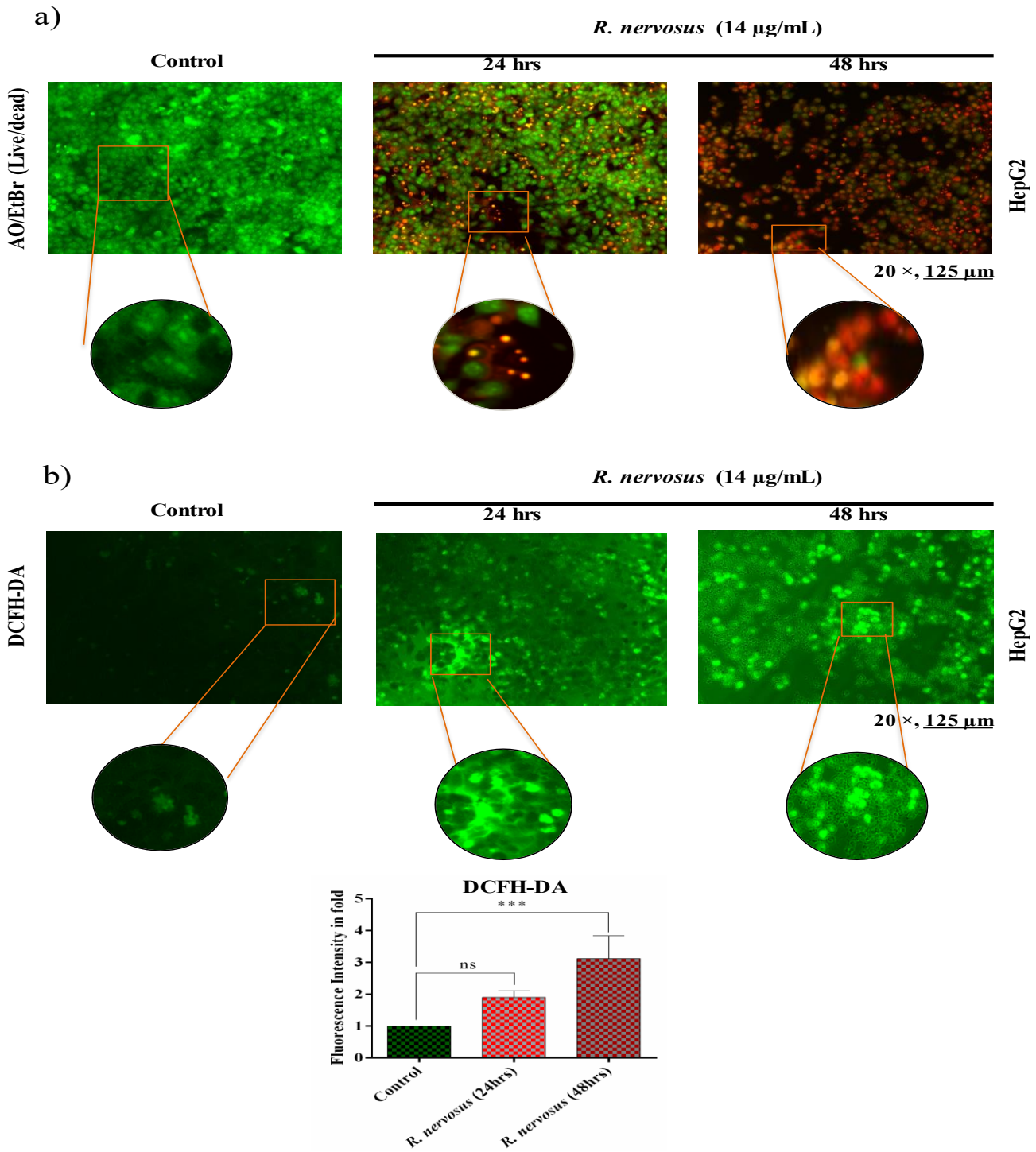

Fig. 2. *R. nervosus* generates intracellular ROS and dead material: a)Represents the morphological damages by *R. nervosus* through acridine orange/ ethidium bromide staining method and control cells exhibit the compact nuclei with good cytoplasm with high green emission. The 24 and 48 hrs treated cells stained as red emission and observed as damaged cytoplasm. b) Illustrated the intracellular generation of ROS. Control cells emit lower green emissions compared with *R. nervosus*-treated. ROS quantification level was detected by the spectrofluorometric method. All quantified values represent mean ± SD. Statistical significance is performed by one-way ANOVA followed by Dunnett's multiple comparison test. Values are statistically significant at ***$p<0.001$, and *ns*.

MMP loss and DNA fragmentation under *R. nervosus* administration: *R. nervosus* effectively deregulated cell viability. Keeping this in mind, this study analysis the mitochondria membrane potential and DNA fragmentation. The results revealed that untreated cells showed that higher emission of green fluorescence rather than treated cells exhibit a lower amount of green fluorescence. That acknowledges the loss of mitochondrial potential loss in HepG2 cells (Fig. 3a). In consideration of DNA fragmentation, *R. nervosus* induces DNA degradation under 24 and 48 hrs treated cells and the instability of DNA caused by *R. nervosus* (Fig. 3b). The spectrofluorometric analysis reflects the same observation for MMP loss and DNA fragmentation (Fig. 3c and d).

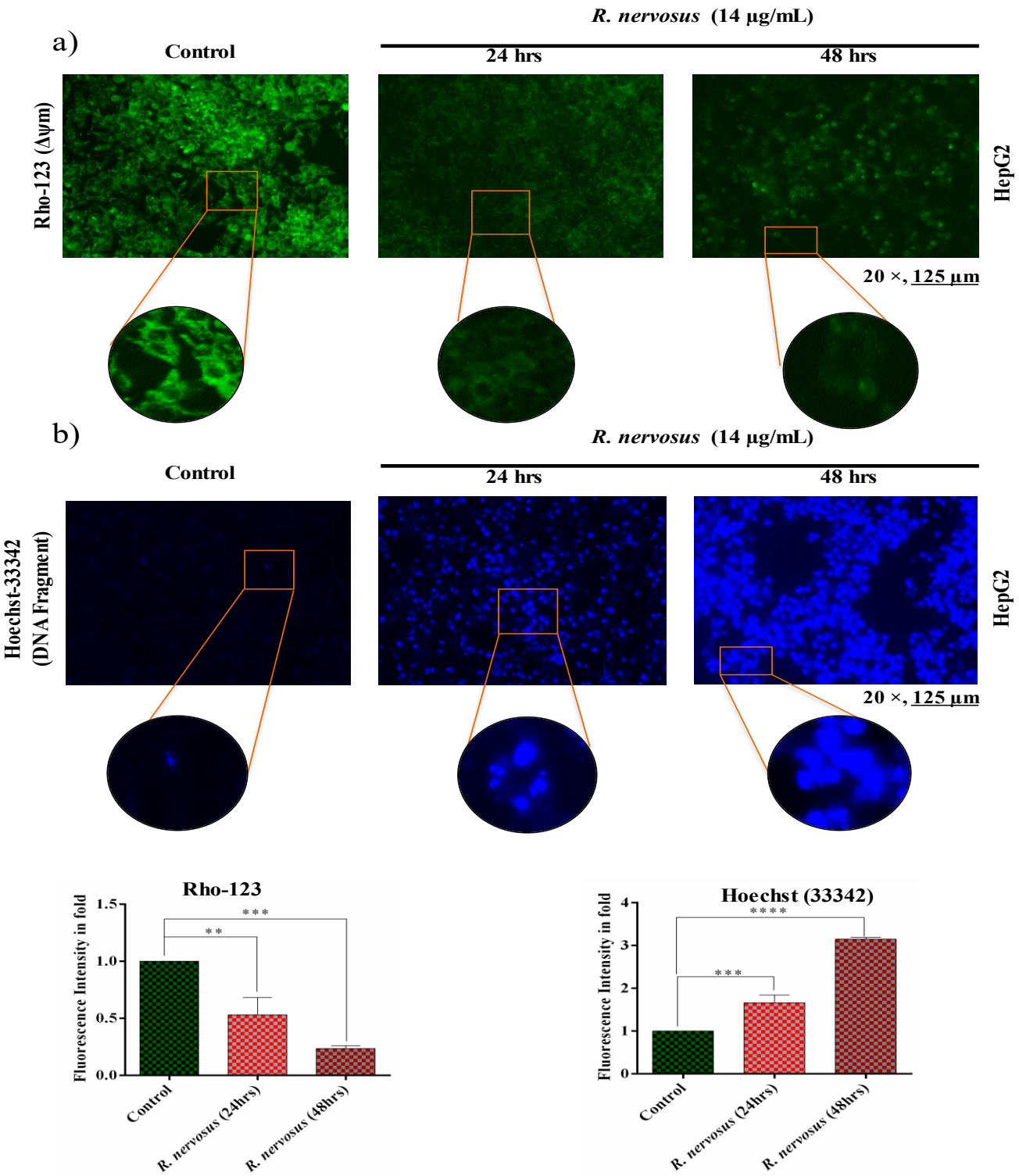

Fig. 3. Effect of *R. nervosus* on MMP (ΔΨm) and DNA fragmentation:a) The images illustrated the mitochondrial membrane potential against the *R. nervosus*. Control cells emit the green color significantly while lower emission of *R. nervosus*-treated cells at 24 and 48 hrs. The quantification data reflect the same pattern of emission. b) Hoechst staining on HepG2 cells after treatment with and without *R. nervosus*. Control emits a very lower blue emission. Contrarily, treated cells emit a higher amount of blue and it denoted highly fragmented founded in HepG2 cells. The respective quantification data reflects the obtained results. All quantified values represent mean ± SD. Statistical significance is performed by one-way ANOVA followed by Dunnett's multiple comparison test. Values are statistically significant at ****p<0.0001, ***p<0.001, and **p<0.01.

Determination of cell esterase under *R. nervosus* in HepG2 cells: The FDA assay was carried out to confirm the cell esterase activity and prove the cell viability loss. Briefly, cell esterase activity was suppressed in the *R. nervosus* treated HepG2 cells. 24 and 48 hrs treatment cells showed minimal green emission compared with control cells (Fig. 4a). The reduced level of cell esterase acknowledges cell death under ethanol extraction of *R. nervosus* administration in HepG2 cells.

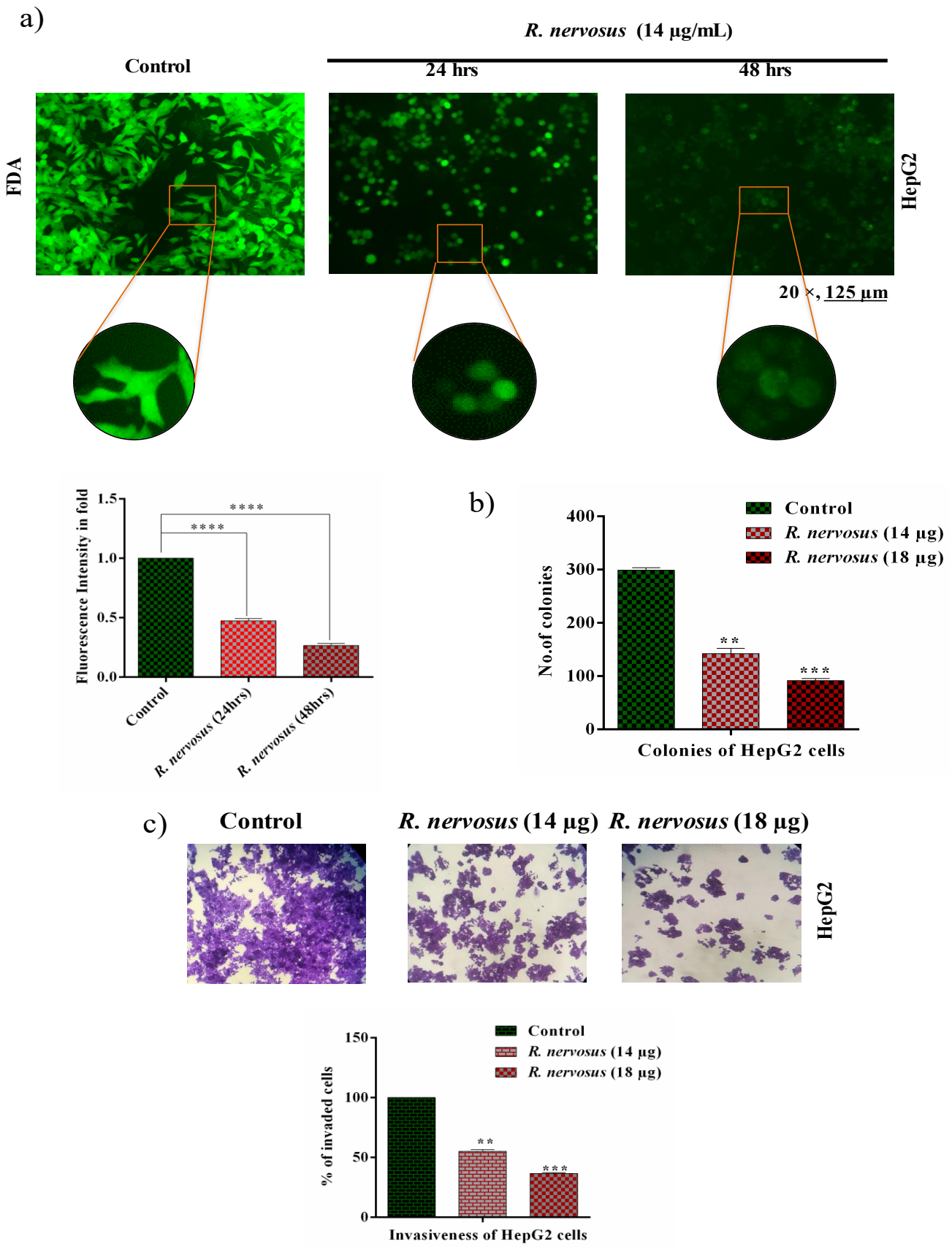

Fig. 4. Effect of *R. nervosus* on cell viability (esterase activity), colony formation, and invasion of HepG2: a) Represents the FDA staining on *R. nervosus* treated and untreated HepG2 cells. Control cells showed a higher emission of green color while observing the minimal emission of green in treated cells. The quantification expresses the same results. b) The graph shows colony formation results treated upon *R. nervosus*. c) Invasion property of HepG2 cells was tested against *R. nervosus,* and the graph illustrated the same results. All quantified values represent mean ± SD. Statistical significance is performed by one-way ANOVA followed by Dunnett's multiple comparison test. Values are statistically significant at ****p<0.0001, ***p<0.001, and **p<0.01.

Impact of *R. nervosus* on colony formation and cell invasion: Colony formation assays revealed that *R. nervosus* significantly suppressed the ability of HepG2 cells to form colonies (Fig. 4b). Matrigel-coated invasion assays further showed that *R. nervosus* inhibited cell invasion in a dose-dependent manner (Fig. 4c). Collectively, invasion and colony formation abilities were reduced under the treatment upon the *R. nervosus* administration.

***R. nervosus* significantly arrest HepG2 cell migration:** Wound healing assays at 0, 12, 24, and 48 hours demonstrated that control cells exhibited progressive wound closure. In contrast, *R. nervosus*-treated cells showed impaired migration, with the wound area remaining unhealed or enlarged. This indicates that *R. nervosus* effectively inhibits HepG2 cell migration (Fig. 5a).

***R. nervosus* upregulates caspase-3& 9:** This indicates that *R. nervosus* effectively inhibits HepG2 cell migration. This upregulation pattern suggest that *R. nervosus* consistently induces the caspase cascade for the promotion of cellular apoptosis (Fig. 5b and c).

Apoptotic and angiogenic gene expressions under *R. nervosus*: *R. nervosus* treatment upregulated apoptotic genes (caspase-3, -8, -9), pro-apoptotic genes (Bid, Bax), and cytochrome c (CYCS), while downregulating the anti-apoptotic gene Bcl2 and PARP expression. The PI3K/Akt pathway was disrupted, showing downregulation of PI3K and Akt (Fig. 6a and b). These findings indicate that *R. nervosus* deregulates cell survival pathways by modulating apoptotic regulators.

***R. nervosus* effect on apoptotic and angiogenic protein expressions:** Immunoblot analysis showed elevated cytochrome c and cleaved PARP levels in *R. nervosus*-treated cells, indicating ETC disruption and impaired DNA repair. Additionally, p-Akt levels decreased significantly, confirming loss of cell survival signaling. VEGFA levels were suppressed, while HIF-1α was upregulated (Fig. 6c). These results confirm that *R. nervosus* promotes apoptosis and suppresses angiogenesis in HepG2 cells.

Discussion

Medicinal plants are composed of potentially bioactive compounds and medicinal plant-based therapy significantly produces anti-cancer results in clinical trials (Hosseini & Ghorbani, 2015). This study focused on investigating the anti-cancer activity of the *R. nervosus* plant against hepatocellular carcinoma. *R. nervosus* is a perennial medicinal plant found in Saudi Arabia including the horn of Africa. particularly in the Sarawat Mountains. Traditionally, all parts of this plant have been used to treat numerous infections (Desta *et al*., 2015).

Research on *R. nervosus* extraction remains limited. Particularly, Getie *et al*., (2003) demonstrated that leaf extracts of *R. nervosus* posses antibacterial effect, although no anti-fungal properties were observed. Additionally, Qasem *et al*., (2020) highlighted that the *R. nervosus* leaf extract effectively treated *Eimeria tenella*-infected chickens, aiding in the recovery of damaged goblet cells, which highlights its anticoccidial potential. This result confirms that *R. nervosus* exhibited a good anti-coccidial effect among the poultry chicken population. In another study, methanol leaf extract of R. nervosus demonstrated anti-diabetic effects in diabetic nephropathy-induced rats, potentially through the activation of the Nrf2 signaling pathway and antioxidant mechanisms (AlMousa *et al*., 2022a). These experimental results could state that methanol-based leaf extraction of *R. nervosus* proves the anti-diabetic potential. Moreover, methanol and n-hexane-based extraction of different parts of the *R. nervosus* showed potent anti-bacterial and fungal activity (Al Yahya *et al*., 2018). Most recently, AlMousa *et al*., (2022b) further confirmed an anti-microbial and anti-oxidant experiment (DPPH) depending on a methanol extraction of *R. nervosus* leaves. They recorded the remarkable anti-oxidant and antibacterial effects against significant pathogens particularly, against Gram-positive bacteria (AlMousa *et al*., 2022b). More on, Qaid *et al*., (2022) reported that dietary supplementation with powdered *R. nervosus* leaves reduced oocyst levels in Eimeria tenella-infected birds, reinforcing its anticoccidial activity.

Despite these findings, research on the anti-cancer potential of *R. nervosus* remains sparse. Quradha *et al*., (2019), evaluated crude leaf extraction and essential oil against against various cancer cell lines, reporting significant cytotoxicity against breast cancer cells (MCF-7 and MDA-MB-231) IC_{50} values of 20.5138 ± 0.933 and 25.1728 ± 0.9176 respectively. However, the essential oil showed limited efficacy against Hela and 3T3 cells. To address this gap, our study explored the effects of ethanol extracts of *R. nervous* on HepG2 cells, demonstrating significant cytotoxicity and induction of apoptosis. These results are coherent with Pfeffer *et al*., (2018), who reported that similar outcomes in hepatocellular carcinoma cell lines. We observed that *R. nervosus* extract inhibited HepG2 cell migration, a critical process for angiogenesis and metastasis. This observation supports the findings of Gupta & Qin (2003), who noted the importance of migration inhibition in preventing tumor progression. Furthermore, our results revealed that *R. nervosus* extract suppressed the invasive potential of HepG2 cells through matrigel barriers, indicating its potential to inhibit tumor angiogenesis (He *et al*., 2022). Suppression of colony formation further corroborated the loss of cell viability and the induction of apoptosis (Backer *et al*., 2011). At the molecular level, we significant overexpression of caspase-3 mRNA, a key apoptotic marker. Enhanced caspase-3 expression is associated with therapeutic efficacy in cancer treatment (Boudreau *et al*., 2019). Dysregulation of caspases, including caspase-9 and caspase-8, is linked to various cancers, and their activation can resensitize chemoresistant cells (Li *et al*., 2017; Fianco *et al*., 2018). Our data also showed the suppression of anti-apoptotic Bcl2, activation of pro-apoptotic Bax, release of cytochrome c proteins, and cleavage PARP, consistent with established apoptotic pathways (Holdenrieder & Stieber, 2004).

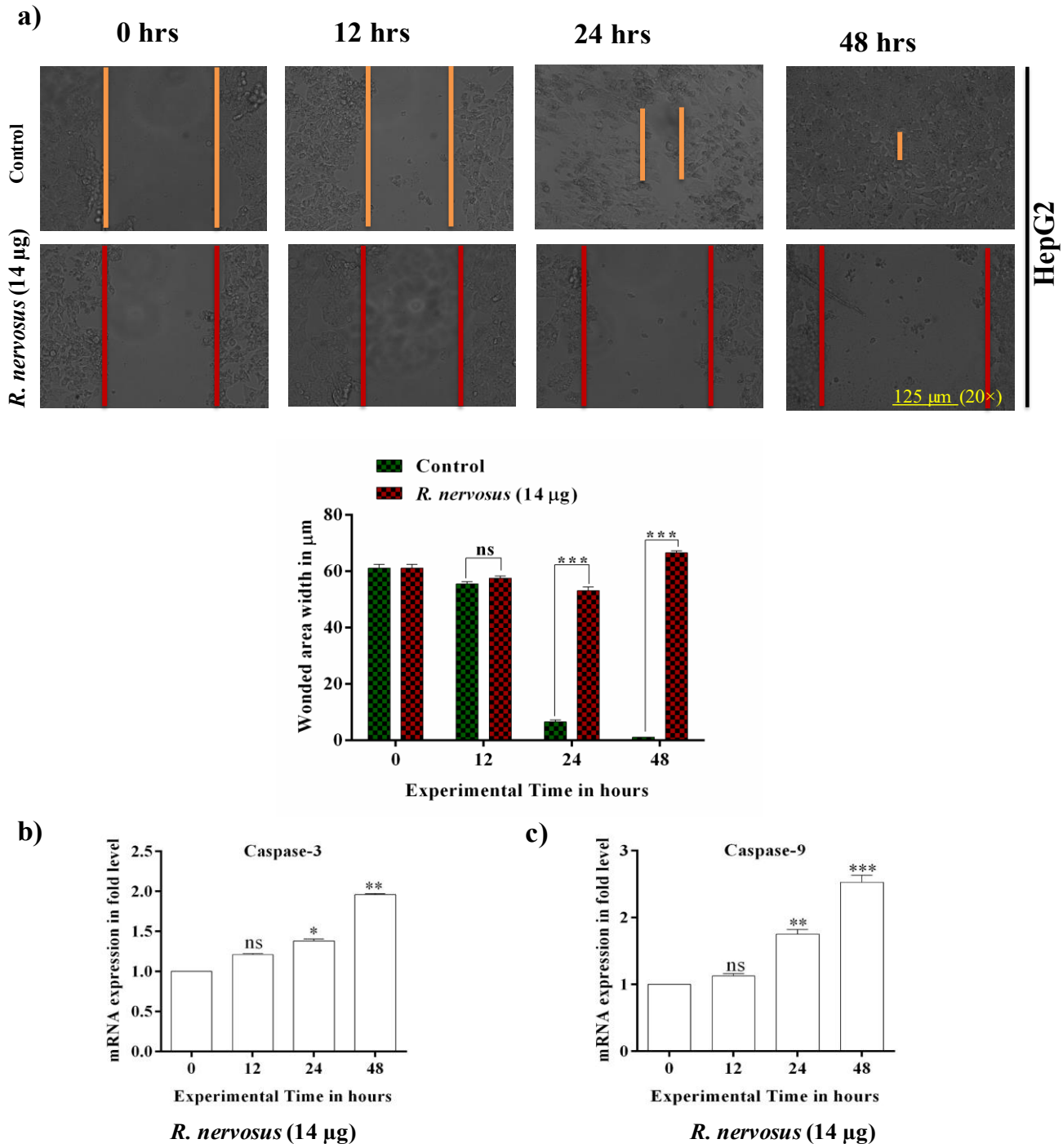

Fig. 5. *R. nervosus* suppress the migration of HepG2 cells and upregulates the caspase-3 & 9 mRNAs: a) The time depended on the experiment of wound healing assay reveals the migration property of HepG2 cells under *R. nervosus* treated and untreated cells. The quantification data summarizes the wound-healing potential. b and c) The mRNA (Caspase-3and 9) expression of R. nervosus treated cells in a time-dependent manner. All quantified values represent mean ± SD. Statistical significance is performed by one-way ANOVA followed by Dunnett's multiple comparison test. Values are statistically significant at ***p<0.001, **p<0.01, *p<0.05, and *ns*.

The cell survival protein, Akt promotes many cellular functions including angiogenesis and cell apoptosis. Numerous signaling pathways are guided by Akt signaling as the central hub and its targeting is a valuable role in cancer treatment (Revathidevi & Munirajan, 2019; Song *et al*., 2019). In addition, PARP inhibitors adequately cause DNA damage by interfering with the DNA repair process. The cleaved product of PARP accepted the hallmarks of cellular apoptosis (Chen, 2011). Our findings suggest that *R. nervosus* extract effectively modulates these pathways. On the other hand, pathological angiogenesis relies on VEGF production within the cancer cells and it initiates the cancer metastasis by augmenting the colony formation in different sites of the body. The targeting of VEGF in cancer treatment may serve as a new modality or rational therapy in cancer (Carmeliet, 2005; Hicklin & Ellis, 2005). (Fig. 7) summarises the overall cellular action of ethanol extraction of *R. nervosus* in inducing apoptosis and arrest angiogenesis in hepatocellular carcinoma cells (HepG2).

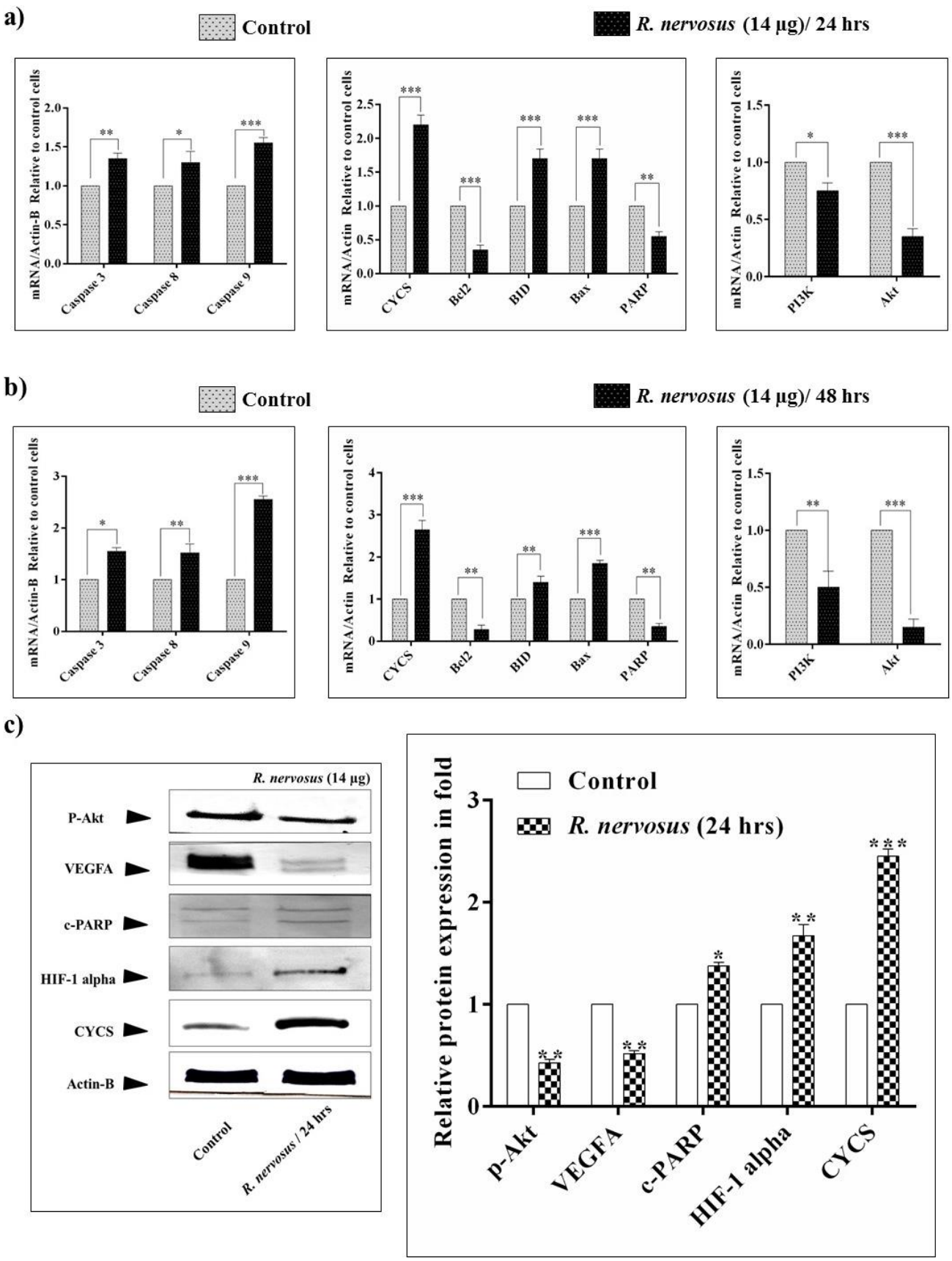

Fig. 6. *R. nervosus* regulates the apoptotic angiogenic genes/ proteins in HepG2 cells: a) The graph represents the qRT-PCR results of apoptosis-regulated genes at 24 and 48 hrs treated upon *R. nervosus*. The qRT-PCR results included caspase-3, 8, and 9; anti-apoptosis gene Bcl2; pro-apoptosis gene BID and Bax; apoptosis marker Cytochrome c (CYCS) and PARP. b) The western blot analysis revealed suppression of p-Akt, and VEGFA while upregulation of cleaved PARP, HIF-1α, and Cytochrome c. All quantified values represent mean ± SD. Statistical significance is performed by one-way ANOVA followed by Dunnett's multiple comparison test. Values are statistically significant at ***p<0.001, **p<0.01, and *p<0.05.

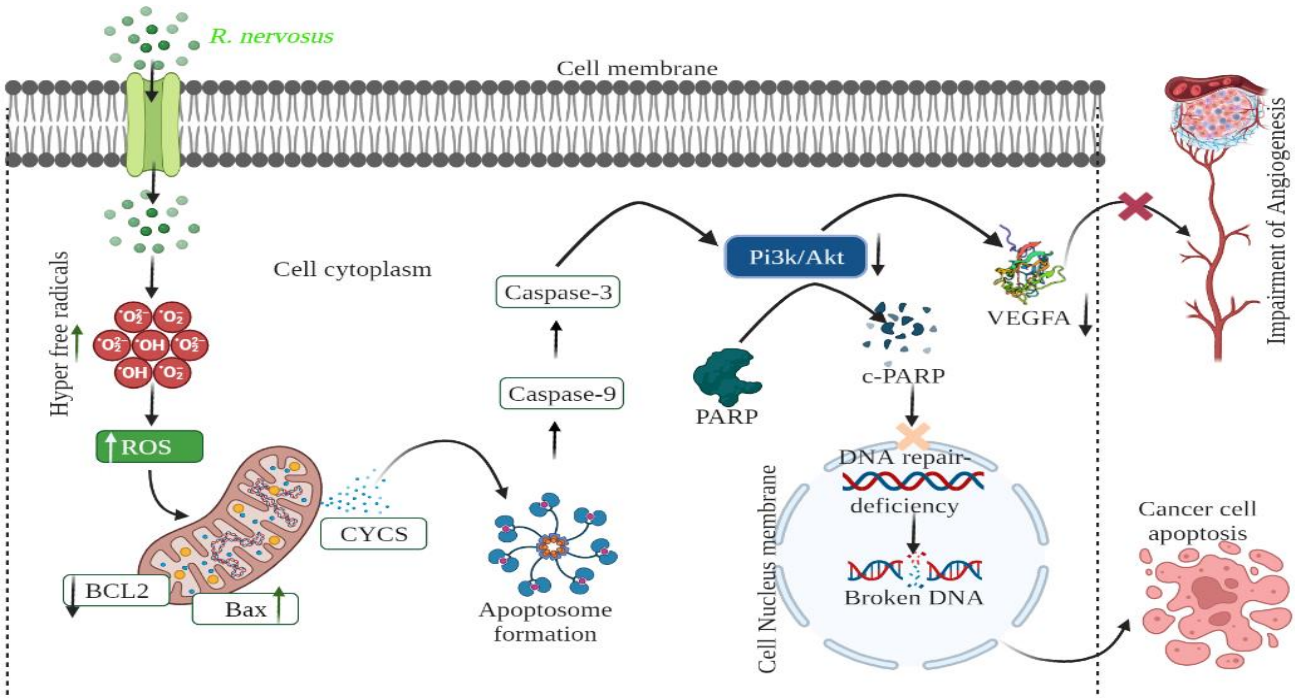

Fig. 7. Schematic representation of the study: Graph illustrated the *R. nervosus* mediated cell death mechanism and angiogenesis arrest in the liver cancer HepG2 cells.

Conclusion

In conclusion, the administration of *R. nervosus* extract demonstrated significant cytotoxicity against HepG2 cells by inhibiting the viability/proliferation of cells. The treatment induced the morphological changes, including cellular collapse, increased ROS production, loss of mitochondrial membrane potential, DNA fragmentation, and formation of apoptotic bodies. In the molecular insights view, *R. nervosus* positively upregulates apoptotic genes including caspase-3, 8, 9, and cytochrome c mRNAs. The pro-apoptotic gene like Bid and BaxmRNAs were significantly upregulated, while the downregulation of anti-apoptotic mRNA Bcl2 was significant along with the downregulation of Pi3k/Akt mRNA. The *R. nervosus* upregulated proteins such as cytochrome c, cleaved PARP, and HIF-1α. On other hand, it significantly suppresses the VEGFA and p-Akt proteins. Altogether, the altered gene networks are effectively reflected in cellular functions such as cellular invasion, migration, and colony-forming arrest. Hence this study suggests that *R. nervosus* might consider a therapeutic agent for hepatocellular carcinoma. However, future research should focus on identifying the specific bioactive phytochemicals responsible for these effects and validating their efficacy through *In vivo* animal studies to advance this promising therapy to the next stage of development.

References

Agarwal, A., R.Z. Mahfouz, R.K. Sharma, O. Sarkar, D. Mangrola and P.P. Mathur. 2009. Potential biological role of poly (ADP-ribose) polymerase (PARP) in male gametes. *Reprod. Biol. Endocrinol.*, 7: 143. https://doi.org/10.1186/1477-7827-7-143

Al Mousa. L.A., N.A. AlFaris, G.M. Alshammari, M.M. Alsayadi, J.Z. ALTamimi, R.I. Alagal and M.A. Yahya. 2022a. *Rumex nervosus* could alleviate streptozotocin-induced diabetic nephropathy in rats by activating Nrf2 signaling. *Sci. Prog.*, 105: 368504221102751. https://doi.org/10.1177/00368504221102751

Al Yahya, N.A., S.A. Alrumman and M.F. Moustafa. 2018. Phytochemicals and antimicrobial activities of *Rumex nervosus* natural populations grown in Sarawat Mountains, Kingdom of Saudi Arabia. *Arab. J. Sci. Engin.*, 43: 3465-3476. https://doi.org/10.1007/s13369-018-3136-z

AlMousa. L.A., N.A. Al-Faris, G.M. Alshammari, ALTamimi, R.I, M.M. Alsayadi, R.I. Alagal and M.A. Yahya. 2022b. Antioxidant and antimicrobial potential of two extracts from *Capparis spinosa* L. and *Rumex nervosus* and molecular docking investigation of selected major compounds. *Saudi J. Biol. Sci.*, 29: 103346. https://doi.org/10.1016/j.sjbs.2022.103346

Al-Naqeb, G. and A. Deen. 2017. The effect of *Rumex nervosus* Vahl leaves on high fat diet-induced hyperglycemia and hyperlipidemia in albino rats. *Int. J. Chem.*, 1: 80-83.

Alwashli, A., M. Al-Sobarry, Y. Cherrah and K. Alaoui. 2012. Anti-inflammatory and analgesic effects of ethanol extract of *Dracaena cinnabari* Balf, as endemic plant in Yemen. *Int. J. Pharm. Biol. Sci.*, 3: 96-106.

Backer, M.V., J.M. Backer and P. Chinnaiyan. 2011. Chapter three - Targeting the unfolded protein response in cancer therapy. In: Conn PM (Ed.), The unfolded protein response and cellular stress, Part C. *Acad. Press*, 37-56. https://doi.org/10.1016/B978-0-12-385928-0.00003-1

Boudreau, M.W., J. Peh and P.J. Hergenrother. 2019. Procaspase-3 overexpression in cancer: A paradoxical observation with therapeutic potential. *ACS Chem. Biol.*, 14: 2335-2348.

Carmeliet, P. 2005. VEGF as a key mediator of angiogenesis in cancer. *Oncology*, 69(Suppl 3): 4-10.

Chen, A. 2011. PARP inhibitors: its role in treatment of cancer. *Chin. J. Cancer.*, 30: 463-471.

Desta, K.T., G.S. Kim, G.E. Hong, Y.H. Kim, W.S. Lee, S.J. Lee, J.S. Jin, A.M. Abd El-Aty, H.C. Shin, J.H. Shim and S.C.

Shin. 2015. Dietary-flavonoid-rich flowers of *Rumex nervosus* Vahl: Liquid chromatography with electrospray ionization tandem mass spectrometry profiling and *In vitro* anti-inflammatory effects. *J. Sep. Sci.*, 38: 3345-3353. doi: 10.1002/jssc.201500737

Desta, K.T., W.S. Lee, S.J. Lee, Y.H. Kim, G.S. Kim, S.T. Kim, A.M. Abd El-Aty, M. Warda, H.C. Shin, J.H. Shim and S.C. Shin. 2016. Antioxidant activities and liquid chromatography with electrospray ionization tandem mass spectrometry characterization and quantification of the polyphenolic contents of *Rumex nervosus* Vahl leaves and stems. *J. Sep. Sci.*, 39: 1433-1441. https://doi.org/10.1002/jssc.201600018

Fianco, G., C. Contadini, A. Ferri, C. Cirotti, V. Stagni and D. Barilà. 2018. Caspase-8: A novel target to overcome resistance to chemotherapy in glioblastoma. *Int. J. Mol. Sci.*, 19: 3798. https://doi.org/10.3390/ijms19123798

Getie, M., T. Gebre-Mariam, R. Rietz, C. Höhne, C. Huschka, M. Schmidtke, A. Abate and R.H.H. Neubert. 2003. Evaluation of the antimicrobial and anti-inflammatory activities of the medicinal plants *Dodonaea viscosa*, *Rumex nervosus* and *Rumex abyssinicus*. *Fitoterapia.*, 74: 139-143. doi: 10.1016/s0367-326x(02)00315-5

Gupta, M.K. and R.Y. Qin. 2003. Mechanism and its regulation of tumor-induced angiogenesis. *World J. Gastroenterol.*, 9: 1144-1155.

He, X., B. Lee and Y. Jiang. 2022. Extracellular matrix in cancer progression and therapy. *Med. Rev.*, 2: 125-139.

Hicklin, D.J. and L.M. Ellis. 2005. Role of the vascular endothelial growth factor pathway in tumor growth and angiogenesis. *J. Clin. Oncol.*, 23**:** 1011-1027.

Holdenrieder, S. and P. Stieber. 2004. Apoptotic markers in cancer. *Clin. Biochem.*, 37: 605-617.

Hosseini, A. and A. Ghorbani. 2015. Cancer therapy with phytochemicals: evidence from clinical studies. *Avicenna J. Phytomed.*, 5: 84-97.

Khadka, S., Y.H. Lin, J. Ackroyd, Y.A. Chen, Y. Sheng, W. Qian, S. Guo, Y. Chen, E. Behr, Y. Barekatain, N. Uddin, K. Arthur, V. Yan, W.H. Hsu, Q. Chang, A. Poral, T. Tran, S. Chaurasia, D.K. Georgiou, J.M. Asara, F.P. Barthel, S.W. Millward, R.A. DePinho and F.L. Muller. 2023. Anaplerotic nutrient stress drives synergy of angiogenesis inhibitors with therapeutics targeting tumor metabolism. *bioRxiv Preprint Service for Biology*., https://doi.org/10.1101/ 2023.05.07.539744

Krock, B.L., N. Skuli and M.C. Simon. 2011. Hypoxia-induced angiogenesis: good and evil. *Genes and Cancer*, 2: 1117-1133.

Li, P., L. Zhou, T. Zhao, X. Liu, P. Zhang, Y. Liu, X. Zheng and Q. Li. 2017. Caspase-9: structure, mechanisms and clinical application. *Oncotarget.*, 8: 23996-24008. DOI: 10.18632/oncotarget.15098

Lowry, O.H., N.J. Rosebrough, A.L. Farr and R.J. Randall. 1951. Protein measurement with the Folin phenol reagent. *J. Biol. Chem.*, 193: 265-275.

Pfeffer, C.M. and A.T.K. Singh. 2018. Apoptosis: A target for anticancer therapy. *Intern. J. Mol. Sci.*, 19: 20448.

Qaid, M.M., L. Mansour, M.A. Al-Garadi, A.H. Alqhtani, A.A. Al-abdullatif, M.A. Qasem and M.A. Murshed. 2022. Evaluation of the anticoccidial effect of traditional medicinal plants, *Cinnamomum verum* bark and *Rumex nervosus* leaves in experimentally infected broiler chickens with *Eimeria tenella*. *Ital. J. Ani. Sci.*, 21: 408-421. https://doi.org/10.1080/1828051X.2022.2033139

Qasem, M.A.A., M.A. Dkhil, E.M. Al-Shaebi, M. Murshed, M. Mares and S. Al-Quraishy. 2020. *Rumex nervosus* leaf extracts enhance the regulation of goblet cells and the inflammatory response during infection of chickens with *Eimeria tenella*. *J. King Saud University, Science*, 32: 1818-1823. https://doi.org/10.1016/j.jksus.2020.01.024

Quradha, M.M., R. Khan, M.U. Rehman and A. Abohajeb. 2019. Chemical composition and *In vitro* anticancer, antimicrobial and antioxidant activities of essential oil and methanol extract from *Rumex nervosus*. *Nat. Prod. Res.*, 33: 2554-2559.

Rahman, A.H.M., M. Anisuzzaman, F. Ahmed, A. Naderuzzaman and A. Islam. 2007. A floristic study in the graveyards of Rajshahi City. *Res. J. Agri. Biol. Sci.*, 3: 670-675.

Revathidevi, S. and A.K. Munirajan. 2019. Akt in cancer: Mediator and more. *Seminars in Cancer Biology.*, 59: 80-91. https://doi.org/10.1016/j.semcancer.2019.06.002

Rohlena, J., L.F. Dong and J. Neuzil. 2013. Targeting the mitochondrial electron transport chain complexes for the induction of apoptosis and cancer treatment. *Curr. Pharm. Biotechnol.*, 14: 377-389. DOI: 10.2174/1389201011314030011

Song, M., A.M. Bode, Z. Dong and M.H. Lee. 2019. AKT as a therapeutic target for cancer. *Cancer Res.*, 79: 1019-1031.

Sung, H., J. Ferlay, R.L. Siegel, M. Laversanne, I. Soerjomataram, A. Jemal and F. Bray. 2021. Global cancer statistics 2020: GLOBOCAN estimates of incidence and mortality worldwide for 36 cancers in 185 countries. *CA: A Cancer Journal for Clinicians.*, 71: 209-249. DOI: 10.3322/caac.21660

Zhou, Y., S. Li, J. Li, D. Wang and Q. Li. 2017. Effect of microRNA-135a on cell proliferation, migration, invasion, apoptosis and tumor angiogenesis through the IGF-1/PI3K/Akt signaling pathway in non-small cell lung cancer. *Cell. Physiol. Biochem.*, 42: 1431-1446. DOI: 10.1159/000479207

(Received for publication 11 October 2024)